

Phase transitions and critical phenomena of tiny grains thin films synthesized in microwave plasma chemical vapor deposition and origin of ν_1 peak

Mubarak Ali ^{a, *} and I-Nan Lin ^b

^a Department of Physics, COMSATS Institute of Information Technology, Islamabad 45550, Pakistan. E-Mail: mubarak74@comsats.edu.pk, mubarak74@mail.com

^b Department of Physics, Tamkang University, Tamsui Dist., New Taipei City 25137, Taiwan (R.O.C.).

Abstract – Different analyses of tiny grains carbon films known as nanocrystalline and ultra-nanocrystalline diamond films have been observed in Raman spectroscopy and energy loss spectroscopy. Carbon atoms reveal several transitions depending on attained electron-dynamics. Those tiny grains of carbon film comprised graphitic state atoms originate one-dimensional structure revealing natural elongation along east west poles and they are the origin of ν_1 peak under Raman spectroscopy. Those tiny grains of carbon film evolved in fullerene state atoms, they are the origin of ν_2 peak. Where tiny grains originate ν_1 peak, it is at low intensity as compared to the ones known in their exceptional hardness because of one-dimensionally elongated atoms where inter-state electron gap becomes almost straight along east west poles. Enhanced field emission characteristics of films resulted is because of uniformly elongated atoms of tiny grains where propagation of photonic current is accelerated. On interacting laser beam to tiny grains carbon film comprised different states of carbon atoms, elongated graphite, lonsdaleite, diamond, fullerene and graphene, intensity of signals recorded at different wave numbers revealing identical trend as resulted under energy loss spectroscopy of the same carbon film.

Keywords: Tiny grains carbon films; Photon energy; Heat energy; Phase transition; Raman spectra; Energy loss spectroscopy

1.0 Introduction

Development of selective size and shape materials and investigating their characteristics at nanoscale requires a new sort of observations. Phase transition of carbon atoms in tiny grains carbon film is an usual phenomenon but crucial to categories where it may be the origin of different characteristic not yet disclosed. It has been discussed that switching dynamics in carbon films under varying process conditions where growing tiny grains evolve into different morphology [1].

The syntheses of nanocrystalline diamond (NCD) and ultrananocrystalline diamond (UNCD) films only span over few decades where interplay of varying process conditions in the presence of different concentrations of feed gases (methane, hydrogen and argon, etc.) while employing technique known as microwave plasma chemical vapor deposition (MPCVD) are the source of their development. The characteristics of NCD/UNCD films are mainly recognized in terms of their microscopic observations, Raman spectroscopy and energy loss spectroscopy, whereas, their performance is mainly recognized in terms of field emission characteristics. The NCD/UNCD films mainly deal tiny grains, size range from tens of nanometer to few nanometers.

It is necessary to understand dynamics of tiny particles' formation prior to go for assembling into large size particles [2]. Agglomerations of colloidal matter envisage atoms and molecules to deal them as materials for tomorrow [3]. Dynamics of formation of different tiny particles have been discussed elsewhere [4]. The formation mechanism of tiny shaped particles under certain concentration of gold precursor has been discussed [5]. Under identical process parameters, the nature of precursor directs tiny shaped particles following by large shaped particles where role of atomic nature is crucial [6]. Different tiny shaped particles were developed under the nano shape energy while varying the ratio of bipolar pulse OFF to ON time [7]. Triangular-shaped tiny particles synthesized directly under unipolar pulse ON/OFF time and a certain structure evolved under the combined application of fundamental forces and nano shape energy [7]. Formation process of large-sized particles reveals very high development rate and diffusion process of atoms of tiny-sized particles is under the stretching of energy knots clamping electron states [8]. In all suitable metals and semimetals, the binding of atoms takes place as per shaping of energy under execution of their electron-dynamics [9]. Tiny shaped particle dealing localized gravity on development of mono layer of developing large shaped particle at solution

surface where its fundamental mechanism of formation along with elongation has been discussed elsewhere [10]. Atoms of suitable elements which execute electronic transitions don't ionize, deform or elongate while inert gas atoms split under the application of photonic current [11]. The phenomena of heat and photon energy have been discussed while dealing silicon atom where under inter-state electron-dynamics heat energy was being configured into photon energy [12]. Influence of chamber pressure has been studied while depositing carbon films in hot-filaments deposition system [13]. Under normal conditions, certain nature atoms formed tiny particles deal deformation and elongation behaviors at greater extent which can work either effective nanomedicine or defective [14].

Electron field emission (EFE) device fabricated by heating tiny diamond grains in hydrogen plasma reveals high characteristic and is due to the high defect density and low electron affinity [15]. Increasing nitrogen content slightly increases sp^2 -bonding in grain-boundary and local bonding structure remains the same [16]. Diverse geometries coupled with varieties of attachment sites enabling diamondoids as useful building blocks for molecular-design applications [17]. Size of grains in UNCD film in the range of 2-3 nm remains thermodynamically stable as tested under broad range of pressure –temperature of hydrogenated surfaces [18]. Grains in nanometer size indicate specific changes because of the decreased mobile dislocations and below their critical size, a softening behavior is often observed, and change is triggered by atomic shuffling where simulations approaches are incapable to evaluate underlying mechanism [19]. Sumant *et al.* [20] investigated the surface chemistry and nanotribology inside the UNCD films and are indistinguishable chemically, adhesively and tribologically from single-crystal diamond.

Several studies of UNCD films are available in the literature targeting field emission characteristics under different process parameters along with varying concentration of gases (and dopants as well). On increasing the local density of states, UNCD films provide conducting path at diamond-vacuum interface [21]. UNCD films synthesized at low temperatures and in nitrogen environment demonstrated high conductivity in their various applications [22]. Under nitrogen atmosphere, the grain size of UNCD film becomes smaller than 10 nm and metallic conductivity is achieved [23]. UNCD film has low friction/wear and rapid passivation of dangling bonds is a matter of concern in humid environment [24]. UNCD films are different as compared to NCD films in several ways such as their grain sizes are 2

nm to 5 nm, they are bound by sp^2 -carbon and usually grow in argon-rich/hydrogen-poor CVD environment and may contain 95–98% sp^3 -bonded carbon [25]. In UNCD films, homojunction facilitates the tunneling of electrons in conduction band and their direct transport at conducting/insulating interface [26]. To synthesize diamond films at temperatures below 600°C, UNCD films are superior in choice because their properties don't degrade as in polycrystalline diamond films [27]. On increasing substrate temperature along with hydrogen concentration in Ar/CH₄ plasma, sp^3 -diamond phase becomes less passivated [28]. Low friction coefficient of UNCD films is linked with large amounts of hydroxylic/carboxylic functional groups which are recognized as grain boundary [29]. Bias enhanced nucleation/growth processes facilitate the transport of graphitic phase in both interior and interface regions of UNCD films [30]. Hydrogen concentration increases the size of diamond grains [31]. Boron-doped UNCD films are capable of being utilized in the field of atomic force microscopy/robust electrodes/bio-compatible sensors [32]. On lowering the a-C layer at interface UNCD/Au-Si composite structure delivers better conductivity and improves EFE [33]. Precise growth of sub-2 nm/above 5 nm sized diamond grains is achieved due to energetic species under low growth temperature and pre-nucleated interface, thus, tiny grains on silicon nanoneedles deliver enhanced EFE [34]. Gold-UNCD films show superior EFE properties than copper-UNCD films and authentic factor underneath the mechanism is the presence of nanographitic phases [35]. Copper ion implantation and annealing process increase the EFE due to the improved conducting nature of UNCD films [36]. Presence of graphitic phases at the interfaces of ZnO nanorods/UNCD needles decreases the resistivity of layer and core-shell heterostructures, thus, delivered superior EFE [37]. Nitrogen-incorporated UNCD grains serve as 'high-density diamond nuclei' in the hybrid carbon film [38]. In all those studies and many others, factors related to performance of UNCD/NCD films are linked with the tiny grains of UNCD/NCD films. Improvement in the conductivity but not EFE of P-ions incorporated-UNCD films was due to the transportation of electrons crossing interface [39]. Transportation of electrons is the prime reason for enhanced conductivity and emission properties of doped UNCD films [40].

Both Raman spectroscopy and energy loss spectroscopy analyses of 'tiny grains carbon films' reveal different peaks of varying intensity along with different trend. Additionally, a film synthesized under the same parameters show different

information of obtained data at different locations. These indicate that 'tiny grains carbon films' deal miscellaneous behaviors of their structure. In the present work, different 'tiny grains carbon films' are synthesized in MPCVD. Formation process of 'tiny grains carbon films' is discussed under the variation of chamber pressure and different concentration of hydrogen gas. Different structures of tiny grains in their films are discussed where atoms deal different electron-dynamics to introduce different phase or state within the same film. Raman spectroscopy and energy loss spectroscopy of 'tiny grains carbon films' tally each other along with their field emission characteristics. The performance of carbon films in terms of tiny grains comprised elongated atoms having structure of smooth elements is pinpointed. In addition to those, confusion has been going on since three decades regarding the origin of peak related to ' ν_1 band' in Raman spectra and it was due to the size of the grains or the presence of transpolyacetylene layers around tiny grains. Present study indicates the real reason of the peak related to ' ν_1 band'.

2.0 Experimental details

To synthesize 'tiny grains carbon films', MPCVD technique (IPLAS-Cyrannus, 2.45 GHz) was employed. A schematic of MPCVD set up have been shown elsewhere [41]. Silicon wafers N-type nature, resistivity $\sim 1-5$ (Ohm-cm), were used as the substrate material. Initial duration of the process (at nucleation stage) was set 30 minutes, whereas, deposition time was set 60 minutes, in each experiment. Prior to load the samples in the chamber, substrates were cleaned by ultrasonic agitation for the duration of 30 minutes in methanol solution containing nanodiamond powders size ~ 30 nm and titanium powders of 325 meshes to create nucleation sites. The total mass flow rate was 200 sccm and was kept constant in each experiment. The substrate temperature was measured by K-type thermocouple where 6 % H_2 in argon –rich methane mixture was used to synthesize carbon films and the recorded value was $700^\circ C \pm 10^\circ C$, whereas, the temperature was significantly lowered in films synthesized without H_2 where recorded value was $500^\circ C \pm 10^\circ C$. On increasing chamber pressure from 100 torr to 200 torr at constant microwave power 1400 (watts), no remarkable difference in temperature was noted. Due to lower thermal conductivity of Ar than H_2 , heating of substrate by plasma is greatly reduced in argon-rich CH_4 mixture [22]. Surface morphology of 'tiny grains carbon films' were analyzed by scanning microscope (FE-SEM, ZEISS Model: SIGMA). Peaks related

to different state of carbon atoms (tiny grains) were identified by Raman spectroscopy (Renishaw; 325 nm and HR800 UV; 632.8 nm). Photon field emission (PFE) characteristics known as electron field emission characteristics of 'tiny grains carbon films' were deduced by using a tunable parallel plate set-up known in $I - V$ curve and measurements were made by employing an electrometer (Keithley 237) under vacuum level of 10^{-6} torr. Dark field, bright field, high-resolution images and selected area photon reflection (SAPR) patterns (known as SAED patterns) of 'tiny grains carbon films' were taken by high-resolution transmission microscope (HR-TEM, JEOL JEM2100F) operated at 200 kV. Energy of different bands in 'tiny grains carbon films' was deduced by core loss photon energy loss spectroscopy (core loss PELS) and low loss photon energy loss spectroscopy (low loss PELS) known as core loss EELS and low loss EELS.

3.0 Results and discussion

Surface morphology of carbon films of various size and shape of tiny grains synthesized at different chamber pressures are shown in Figures S1 (a) to S1 (c); at 150 torr, more tiny grains are in needle-like shapes. In films synthesized at 100 torr and 200 torr, tiny grains are composed more like in the shape of tiny clusters. Morphological features of tiny grains in film synthesized without H_2 gas (Figure S2) are like the ones in film synthesized at 6 % H_2 (Figure S1b). Raman spectra of different films synthesized at 100 torr, 150 torr and 200 torr are shown in Figure 1 revealing different intensity levels of peak related to ' ν_1 band'. The ' ν_1 band' in films synthesized at 100 torr and 200 torr is more pronounced as compared to the ' ν_1 band' in film synthesized at 150 torr. The ' ν_1 band' is intensive in film synthesized without H_2 gas (Figure S3) as compared to the films synthesized at 6% H_2 (Figure 1). In different Raman spectra, the peak related to ' ν_1 band' is at low level of intensity as compared to D^* , D and G peaks. Field emission current density (in known units) as a function of applied field (in known units) at various chamber pressures is shown in Figure 2. Film synthesized at 100 torr shows superior field emission properties where 'turn on field' is 11.52 V/ μ M (the lowest value) and the large current density (> 2.0 mA/cm²). The 'turn on field' was the highest (25 V/ μ M) in the film synthesized at 150 torr, whereas, it is recorded 16.4 V/ μ M at 200 torr.

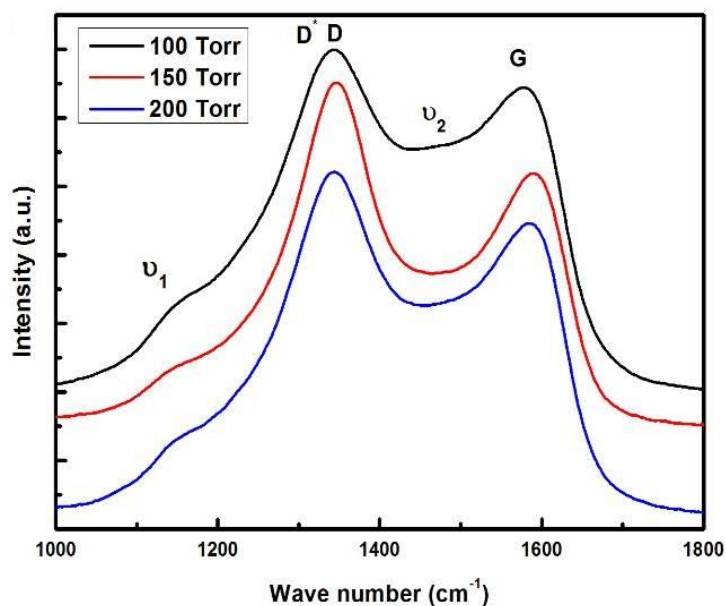


Figure 1: Raman spectra of 'tiny grains carbon films' synthesized at chamber pressure 100 torr, 150 torr and 200 torr; total mass flow rate: 200 sccm (6% H₂, 1 % CH₄ and 93 % argon, Ar: CH₄: H₂ = 186:2:12), microwave power: 1400 (in watts) and deposition time: 60 minutes.

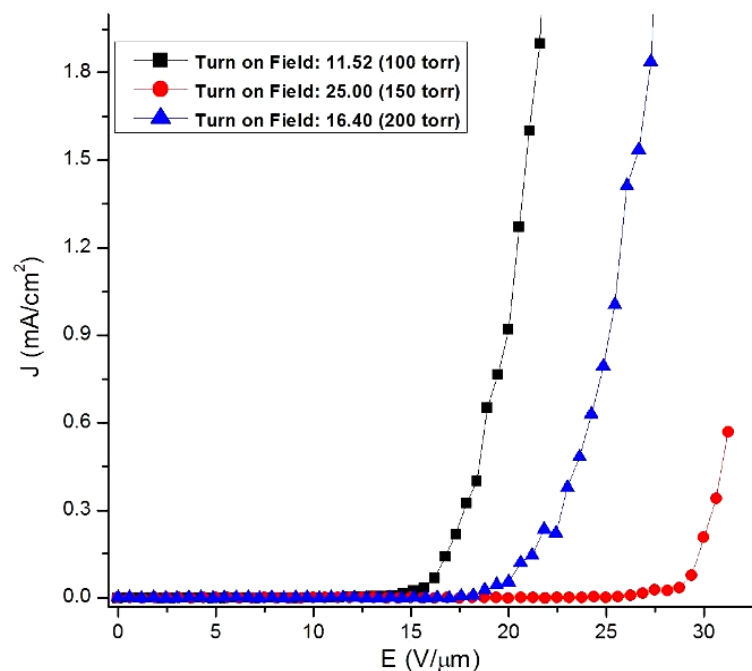


Figure 2: Field emission current density of 'tiny grains carbon films' synthesized at chamber pressure 100 torr, 150 torr and 200 torr as a function of applied field; total mass flow rate: 200 sccm (6% H₂, 1 % CH₄ and 93 % argon, Ar: CH₄: H₂ = 186:2:12), microwave power: 1400 (in watts) and deposition time: 60 minutes.

Field emission current density of different 'tiny grains carbon films' synthesized in Ar-rich CH₄ mixture without H₂ and with H₂ (3% and 6%) as a function of applied field are shown in Figures S4 (a-c). In Figures S4 (a) to S4 (c), the general trend of the

'turn on field' is more morphology-dependent; the value of 'turn on field' at 100 torr is lower than that at 150 torr (same trend in Figure 2). Under lower chamber pressure (at 100 torr), all films in Figure S4 (a-c) show lower 'turn on field' where more number of tiny grains elongated structure to structure of smooth elements as low 'turn on field' value was measured due to enhanced and accelerated propagation of photonic current, whereas, the large value of 'turn on field' in film synthesized at 200 torr (Figure S4a) is appeared to be related to elongation of less number of tiny grains to structure of smooth elements.

Dark field transmission microscope images of 'tiny grains carbon films' synthesized at 100 torr and 200 torr are shown in Figures S5 (a) and S6 (a) where small-sized dark spots are related to isolated tiny grains and bigger dark spots are related to coalesced (packed) tiny grains and contrast is more visible in bright field transmission microscope images shown in Figures S5 (b) and S6 (b); in some regions of the film, tiny grains amalgamated and in some regions of the film, tiny grains dispersed. SAPR patterns taken at the same regions of films (shown in Figures S5b and S6b) are shown in Figures S5 (c) and S6 (c) where intensity spots don't show precise rings related to structure and spotted intensity spots in the pattern reveal structure of different state carbon atoms in 'tiny grains carbon films'. As indicated in the marked scale which is nearly a half of the nanometer where photons reflected at the surface of mixed behavior structure don't reveal any specific order in spotted dots of their intensity in both the patterns.

High-resolution transmission microscope image taken from 'tiny grains carbon film' synthesized at 100 torr is shown in Figure 3 (c) and from the figure two regions of magnified images are shown in Figures 3 (a) and 3 (b). In Figure 3 (c), several tiny grains show elongation to structure of smooth elements, which are related to graphite structure where under neutral behavior of carbon atoms perfectly align along the opposite poles of surface format. A further detail of structural evolution in surface format is given elsewhere [9]. In the image shown in Figure 3 (a), the most of underlying tiny grains (also those at the surface) appear to elongate revealing the structure of smooth elements of their atoms. In Figure 3 (b), a single tiny grain is shown aligned perfectly to elongated atoms into structure of smooth elements. In Figure 3 (c), different texture of surface of 'tiny grains carbon film' indicates mix behavior of phase transition of structure of tiny grains where more number of tiny grains transformed into structure of smooth elements.

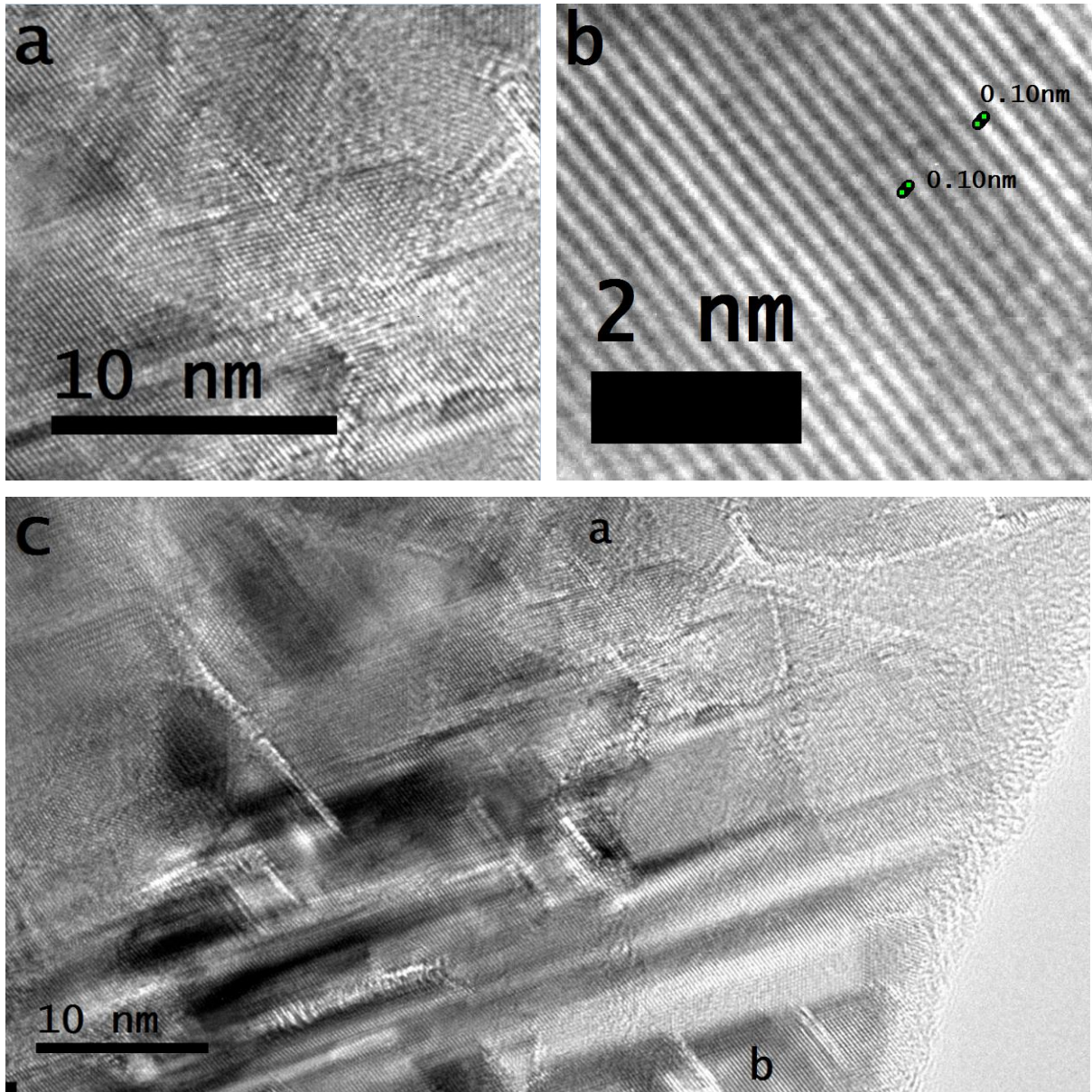


Figure 3: (a) Magnified view of the selected region of high-resolution transmission microscope image shows several overlaid tiny grains, (b) magnified view of the selected region of high-resolution transmission microscope image shows elongated tiny grain of graphite structure and (c) standard high-resolution transmission microscope image shows large number of tiny grains comprised of different state of carbon atoms; 'tiny grains carbon film' synthesized at chamber pressure: 100 torr, mass flow rate: 200 sccm (6% H₂, 1 % CH₄ and 93 % argon), microwave power: 1400 (in watts) and deposition time: 60 minutes.

Figure S7 shows high-resolution transmission microscope image taken from another region of the carbon film, which highlights different features of the tiny grains. Gap between two tiny grains of smooth elements labeled by (2) indicates formation of canal-like channel which is referred as 'graphitic filament' [39, 41]. High-resolution transmission microscope image taken from the carbon film synthesized at

200 torr is shown in Figure 4 (c) revealing different structures of ‘tiny grains carbon film’ and two regions of magnified high-resolution transmission microscope images from the figure are shown in Figures 4 (a) and 4 (b). In Figure 4 (a), the tiny grains other than those elongated to smooth elements are shown but in Figure 4 (b), two tiny grains elongated to structure of smooth elements under the force of opposite poles are shown where a canal-like channel is formed between them. Different texture of surface of ‘tiny grains carbon film’ shown in Figure 4 (c) reveals mix behavior of phase transition of structure of tiny grains where less number of tiny grains transformed into structure of smooth elements.

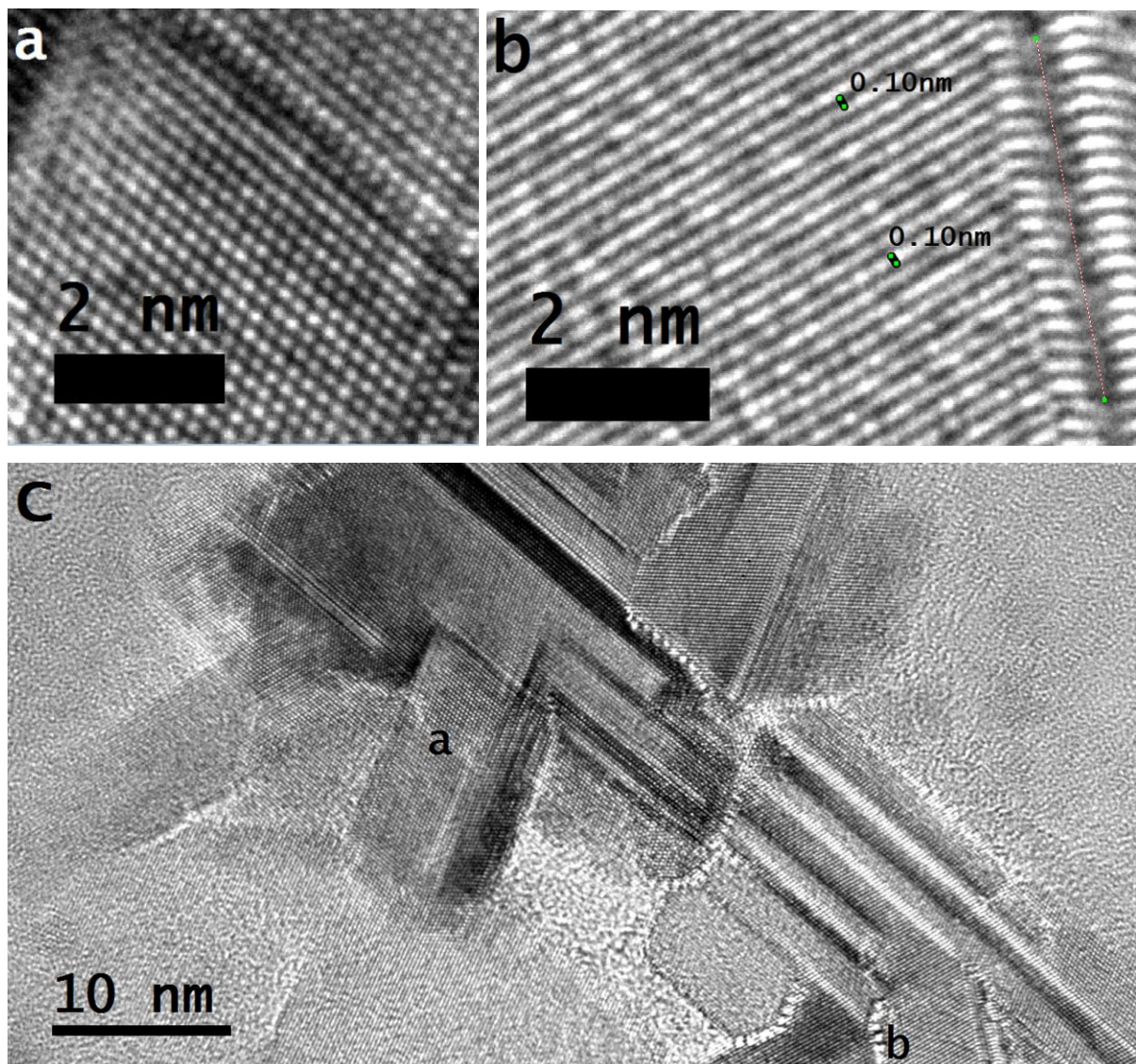


Figure 4: (a) Magnified view of the selected region of high-resolution transmission microscope image shows tiny grain of different state carbon atoms, (b) magnified view of the selected region of high-resolution transmission microscope image shows tiny grain of structure of smooth elements and (c) standard high-resolution transmission microscope image shows several tiny grains comprising

different state of carbon atoms; 'tiny grains carbon film' synthesized at chamber pressure: 200 torr, mass flow rate: 200 sccm (6% H₂, 1 % CH₄ and 93 % argon), microwave power: 1400 (in watts) and deposition time: 60 minutes.

From these high-resolution microscopic images, it is difficult to identify all the different state atoms of carbon along with their tiny grains comprising only few atoms known in their exceptional hardness along with other in poor hardness. Again, where tiny grains of graphite structure don't deal any sort of elongation, they retain other state of atoms. In such 'carbon tiny grains films', propagation of photonic current is accelerated because of the naturally channelized inter-state electron gap. This is the cause of recognition of UNCD/NCD films in terms of enhanced field emission characteristics where inter-state electron gap works efficiently, thus, allowing propagation of accelerated current density of photons wavelength in inter-state electron gap as discussed elsewhere [11]. This reveals that a tiny-sized particle or quantum dots doesn't collectively oscillate on trapping or coupling light (photons). Thus, disregards the largely studied phenomenon of surface plasmon polaritons.

Core loss PELS obtained at the same region of 'tiny grains carbon films' from where high-resolution transmission microscope images were taken as shown in Figures 5 (a) and (b). An abrupt rise near 292 eV referred to σ^* -band and a large dip near 305 eV referred to diamond phase [42, 43] and these bands are also found in the films synthesized at 100 torr and 200 torr as shown in Figures 5 (a) and (b). However, the large dip curve in both films which is more indicative in the case of film synthesized at 200 torr (Figure 5b) is due to energy of band related to tiny grains elongated structure to structure of smooth elements (~ 285 eV). The core loss PELS of both films reveal the same energy peaks related to different bands and identical trend to the one observed in the case of Raman spectroscopy. But in the case of Raman spectroscopy, the peaks' positions were at different wave numbers, whereas, in core loss PELS the peaks' positions are at different energy bands; atoms (or their tiny grains) of films transformed into lonsdaleite, diamond and graphene states are at peak ~ 295 (eV), ~ 308 (eV) and ~ 328 (eV), respectively. Tiny grains remained in fullerene state of carbon atoms revealing the decreasing level of energy in the form of dip curve at band ~ 304 (eV) in both films as notable in Figures 5 (a) and (b). In Figure 5 (a), more pronounced hump-like peaks at ~ 328 eV is due to more atoms (or tiny grains) of films transformed into graphene state.

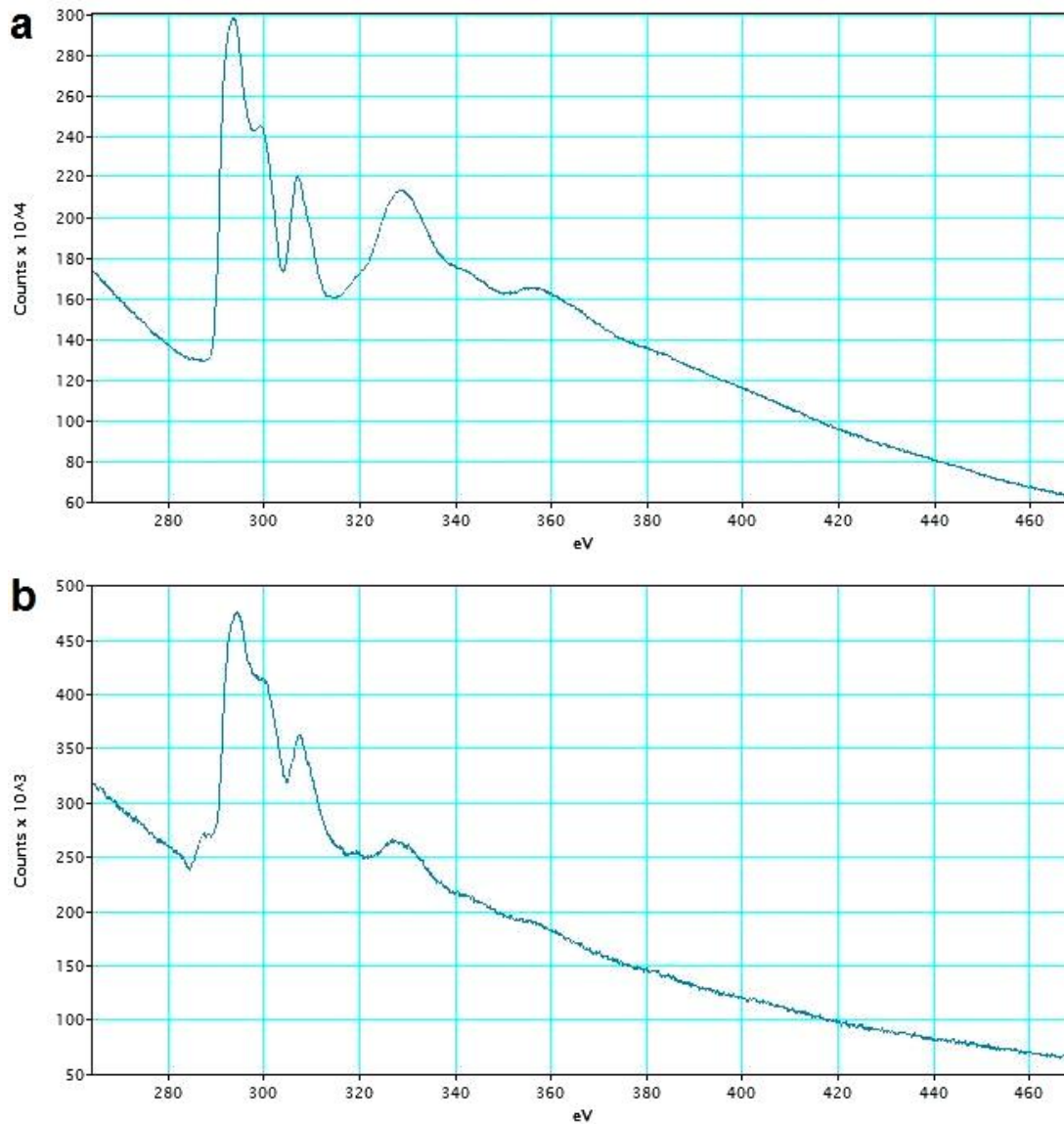


Figure 5: Core Loss photon energy loss spectroscopy (known as core loss EELS) of ‘tiny grains carbon films’ synthesized at chamber pressure (a) 100 torr and (b) 200 torr; total mass flow rate: 200 sccm (6% H₂, 1 % CH₄ and 93 % argon), microwave power: 1400 (in watts) and deposition time: 60 minutes.

In low loss EELS, graphite phase of carbon film shows a prominent peak at s_3 (27 eV), whereas, the a-C phase shows a peak at s_1 (22 eV) [43, 44]. However, in low loss PELS shown in Figures 6 (a) and (b), a peak at 27 eV is not available and band is at slightly titled position instead of being at 22 eV for both ‘tiny grains carbon films’ indicating different trend of atoms of ‘tiny grains carbon films’. Overall, the trend of peaks’ behavior related to different band energy is in the same manner as observed in the case of core loss PELS of these films. The built-in unit (eV) in the case of core loss PELS and low loss PELS are replaced with photon volts (pV).

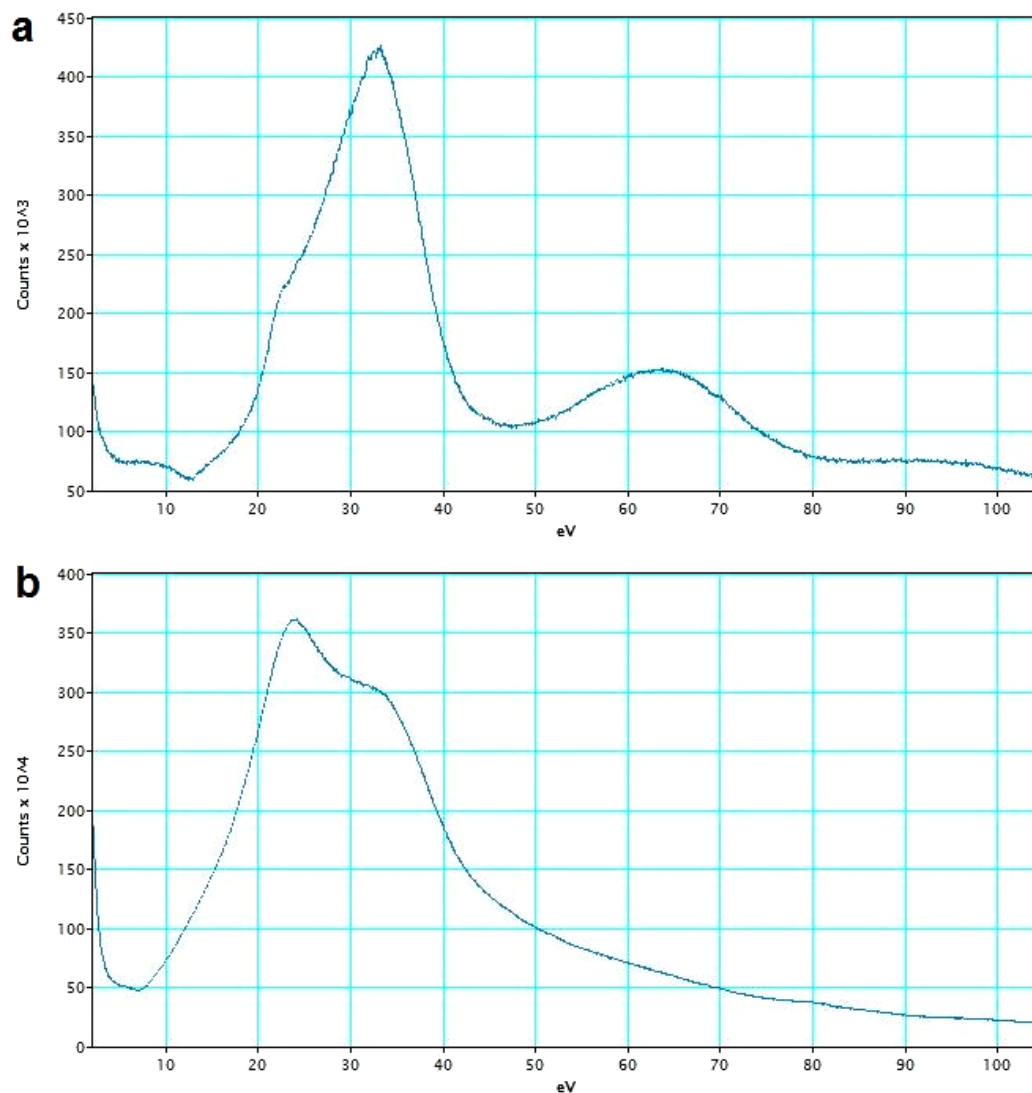


Figure 6: Low loss photon energy loss spectroscopy (known as low loss EELS) of ‘tiny grains carbon films’ synthesized at chamber pressure (a) 100 torr and (b) 200 torr; total mass flow rate: 200 sccm (6% H₂, 1 % CH₄ and 93 % argon), microwave power: 1400 (watts) and deposition time: 60 minutes.

In Raman spectra of NCD/UNCD films, the peak at 1150 cm⁻¹ has been attributed to nanocrystalline diamond [44-46], however, the ν_1 peak (at 1150 cm⁻¹) cannot originate from a nanodiamond or related sp^3 -bonded phase but it is assigned to transpolyacetylene segments at grain boundaries and surfaces [47]. Nemanich *et al.* [45, 46] proposed that 1150 cm⁻¹ peak arises from nanocrystalline or amorphous diamond. In the Raman spectrum of NCD/UNCD film, the sharp peak at 1332.1 cm⁻¹ is the characteristic of diamond and broadening of the peak is related to the NCD grains [48]. In NCD/UNCD films, the peak at 1150 cm⁻¹ appears hypothetically due to CH bonds and is always linked to another peak at 1450 cm⁻¹, and the peaks at 1330 cm⁻¹ and 1560 cm⁻¹ are due to D-band and G-band [49]. However, in the light of

presented results of 'tiny grains carbon films', argon gas increased the rate of re-nucleation and the amount of tiny grains sizes < 10 nm enhanced significantly. Depending on how many tiny grains elongated structure to structure of smooth elements, their quantity experienced Raman laser, the contribution recorded in the form of peak at wave number ~ 1150 cm^{-1} . In microcrystalline diamond films, the size of grains is very large [1], thus, they don't retain graphite structure and diamond state atoms at a large extent evolving structure under the coordination of large amount of atomic hydrogen in HFCVD reactor, accordingly, information put forth by Raman signals rather to record peak at 1150 cm^{-1} , the peak is recorded at 1332 cm^{-1} . Thus, the peak at wave number 1150 cm^{-1} is associated to those tiny grains which were developed in their graphite structure where dealt natural elongation along east west pole. Depending on the amount of tiny grains structure of smooth elements the intensity of ' ν_1 peak' is varied; different intensity of ' ν_1 band' is related to the number of the tiny grains evolved in structure of smooth elements experiencing the Raman laser. Those atoms of tiny grains of evolved fullerene structure become the origin of ' ν_2 peak' in the Raman spectrum. In this way, wherever the ' ν_1 peak' is resulted in the Raman spectrum of carbon films, the ' ν_2 peak' is resulted as well. Incorporating H_2 in Ar-rich CH_4 mixture either eliminates the ' ν_1 band' or it appears with less intensity. Without incorporation of H_2 in Ar-rich CH_4 mixture, peak related to ' ν_1 band' is pronounced as shown in Figure S3. On varying concentration of feed gases, the nature of tiny grains is varied as well, thus, counting different numbers of tiny grains structure of smooth elements which record different intensity of ' ν_1 band' in the Raman spectrum. Again, different intensity of ' ν_1 band' is recorded on dealing Raman signals of different wavelength [50, 51] which is due to dealing different nature of energy by the same 'tiny grains carbon film'.

In Raman spectroscopy, the peaks at different wave numbers are resulted because of the absorption of energy of interacting Raman laser in a different manner owing to different states of atoms (of tiny grains) in a carbon film as shown in Table 1; at wave number ~ 1145 cm^{-1} , the peak (due to ν_1 band) is related to elongated graphite structure tiny grains and at wave number ~ 1310 cm^{-1} , the peak (due to D^* band) is related to atoms (tiny grains) which transformed into lonsdaleite state, and at wave number ~ 1332 cm^{-1} , the peak (due to D band) is related to atoms (tiny grains) transformed into diamond state, and at wave number ~ 1480 cm^{-1} , the peak (due to ν_2 band) is related to atoms (tiny grains) transformed into fullerene state and

finally, at wave number $\sim 1580 \text{ cm}^{-1}$, the peak is related to tiny grains of carbon film transformed to graphene state. In Table 1, wavelength of resulted Raman peaks related to different states of atoms is decreasing at increasing wave number indicating the increase in the frequency under decreasing wavelength. In the case of 'v₁ peak', the lowest energy of the structure resulted for the elongated graphite structure tiny grains in the form of dip curve at ~ 285 (measured in eV) at core loss PEELS, thus, gives the longest recorded wavelength ($\sim 8734 \text{ nm}$) in the Raman spectrum. On the other hand, where atoms (of tiny grains) transformed into graphene state, the highest energy of the structure resulted (~ 328 measured in eV) at core loss PEELS, thus, gives the shortest wavelength in the Raman spectrum ($\sim 6329 \text{ nm}$). The tiny grains work under the lowest energy of the structure and the longest wavelength (shortest wave number) result into accelerated propagation of photonic current as in the case of elongated graphite structure tiny grains, thus, their greater amount available in a carbon film results into enhance the field emission characteristics.

Table 1: A carbon film record Raman peaks and energy peaks at different wave numbers and bands when tiny grains evolved in different structure

Elongated graphite structure	Lonsdaleite structure	Diamond structure	Fullerene structure	Graphene structure
Raman spectroscopy (in cm^{-1})				
$\nu_1 \sim 1145$ (8734 nm)	$D^* \sim 1310$ (7634 nm)	$D \sim 1332$ (7508 nm)	$\nu_2 \sim 1480$ (6757 nm)	$G \sim 1580$ (6329 nm)
Core loss photon energy loss spectroscopy (in eV)				
Dip curve at ~ 285	Peak at ~ 295	Peak at ~ 308	Dip at ~ 304	Peak at ~ 328

As it is tabulated in the Table 1, elongated graphite structure tiny grains give the highest value of wavelength indicating that they are the cause of enhanced field per unit length or area as discussed in the case of field emission characteristics of 'tiny grains carbon films'. In the case of lonsdaleite, diamond and graphene phases, the decreased values of wavelength are resulted. Now the question arises that recorded wavelength in the case of fullerene structure is also between diamond and graphene (in Table 1) but measured hardness is at very low level, however, the peak related to fullerene structure is at very low intensity in the Raman spectrum and we can observe its energy in the form of dip curve in the spectrum of photon energy loss

spectroscopy. The scheme of electrons is different in different state carbon atoms will be discussed in a separate submission, thus, delivered the different response of the coordinated or interacted signals, which is distinctive in graphitic state and then in the case of other states of carbon atoms available in a 'tiny grains carbon film'. Despite the fact, input energy entering 'tiny grains carbon film' was the same for atoms of graphitic state and other different transformed states of the carbon atoms but the resulting outcome varied as per their availability in 'tiny grains carbon film'. These findings solicit to devise science of Raman spectroscopy and energy loss spectroscopy, accordingly.

4.0 Conclusions

'Tiny grains carbon films' synthesized under different conditions evolve graphite structure where it is elongated to structure of smooth elements under opposite force of poles. Tiny grains where graphitic state atoms bind under nearly neutral behavior of attained dynamics elongated while dealing the force of opposite poles at center are the origin of ν_1 peak in the Raman spectrum where the lowest wave number is resulted because of enhanced field emission performance under accelerated rate of current density. In the case of tiny grains where graphitic state atoms transformed into fullerene state, they reveal the origin of ν_2 peak in 'tiny grains carbon film'. Results of field emission measurements of films synthesized at different pressure are in matching to energy loss spectroscopy and Raman spectroscopy. In Raman spectra and energy loss spectroscopy, the peaks related to different wave number and band are related to propagation of input energy through inter-state electron gap of atoms of different carbon states in 'tiny grains carbon film'.

Our experimental results well prove and justify the position of peaks related to different state of carbon atoms and in good agreement to field emission characteristics of differently synthesized 'tiny grains carbon film'. In line with this, present studies set a new horizon in synthesizing, analyzing and evaluating materials at nanoscale, and soliciting reinvestigation of materials' syntheses and their performances both for existing and future applications.

Acknowledgements:

Mubarak Ali thanks National Science Council (now MOST) Taiwan (R.O.C.) for awarding postdoctorship: NSC-102-2811-M-032-008 (2013-2014). Authors wish to

thank Mr. Tsung-Min Chen for assisting films' synthesis and Mr. Chien-Jui Yeh in TEM operation.

References:

- [1] M. Ali, M. Ürgen, Switching dynamics of morphology-structure in chemically deposited carbon films -A new insight, Carbon 122 (2017) 653-663.
- [2] S. Link, M. A. El-Sayed, Shape and size dependence of radiative, nonradiative and photothermal properties of gold nanocrystals, Int. Rev. Phys. Chem. 19 (2000) 409- 453.
- [3] S. C. Glotzer, M. J. Solomon, Anisotropy of building blocks and their assembly into complex structures, Nature Mater. 6 (2007) 557-562.
- [4] M. Ali, I –N. Lin, The effect of the Electronic Structure, Phase Transition and Localized Dynamics of Atoms in the formation of Tiny Particles of Gold, <http://arXiv.org/abs/1604.07144>.
- [5] M. Ali, I –N. Lin, Development of gold particles at varying precursor concentration, <http://arxiv.org/abs/1604.07508>.
- [6] M. Ali, I –N. Lin, Tapping opportunity of tiny shaped particles and role of precursor in developing shaped particles, <http://arxiv.org/abs/1605.02296>.
- [7] M. Ali, I –N. Lin, Controlling morphology-structure of particles at different pulse rate, polarity and effect of photons on structure, <http://arxiv.org/abs/1605.04408>.
- [8] M. Ali, I –N. Lin, Formation of tiny particles and their extended shapes – Origin of physics and chemistry of materials, <http://arxiv.org/abs/1605.09123>.
- [9] M. Ali, Structure evolution in atoms of solid state dealing electron transitions. <http://arxiv.org/abs/1611.01255>.
- [10] M. Ali, The study of tiny shaped particle dealing localized gravity at solution surface. <http://arxiv.org/abs/1609.08047>.
- [11] M. Ali, Atoms of electronic transition deform or elongate but do not ionize while inert gas atoms split. <http://arxiv.org/abs/1611.05392>.
- [12] M. Ali, Revealing the Phenomena of Heat and Photon Energy on Dealing Matter at Atomic level. <https://www.preprints.org/manuscript/201701.0028/>.
- [13] M. Ali, M. Ürgen, Deposition Chamber Pressure on the Morphology of Carbon Films. (Submitted for consideration).
- [14] M. Ali, Nanoparticles-Photons: Effective or Defective Nanomedicine, J. Nanomed. Res. 5 (2017): 00139.

- [15] W. Zhu, G. P. Kochanski, S. Jin, Low-Field Electron Emission from Undoped Nanostructured Diamond, *Science* 282 (1998) 1471-1473.
- [16] J. Birrell, J. A. Carlisle, O. Auciello, D. M. Gruen, J. M. Gibson, Morphology and electronic structure in nitrogen-doped ultrananocrystalline diamond, *Appl. Phys. Lett.* 81 (2002) 2235-2237.
- [17] J. E. Dahl, S. G. Liu, R. M. K. Carlson, Isolation and Structure of Higher Diamondoids, Nanometer-Sized Diamond Molecules, *Science* 299 (2003) 96-99.
- [18] J. Y. Raty, G. Galli, Ultradispersity of diamond at the nanoscale, *Nature Mater.* 2 (2003) 792-795.
- [19] S. C. Tjong, H. Chen, Nanocrystalline materials and coatings, *Mater. Sci. Engineer. R* 45 (2004) 1-88.
- [20] A. V. Sumant *et al.*, Towards the Ultimate Tribological Interface: Surface Chemistry and Nanotribology of Ultrananocrystalline Diamond, *Adv. Mater.* 17 (2005) 1039-1045.
- [21] A. R. Krauss, O. Auciello, M. Q. Ding, D. M. Gruen, Y. Huang, V. V. Zhirnov, E. I. Givargizov, A. Breskin, R. Chechen, E. Shefer, V. Konov, S. Pimenov, A. Karabutov, A. Rakhimov, N. Suetin, Electron field emission for ultrananocrystalline diamond films, *J. Appl. Phys.* 89 (2001) 2958-2967.
- [22] X. Xiao, J. Birrell, J. E. Gerbi, O. Auciello, J. A. Carlisle, Low temperature growth of ultrananocrystalline diamond, *J. Appl. Phys.* 96 (2004) 2232-2239.
- [23] O. A. Williams, M. Nesladek, M. Daenen, S. Michaelcon, A. Hoffman, E. Osawa, K. Haenen, R. B. Jackman, Growth, electronic properties and applications of nanodiamond, *Diam. Relat. Mater.* 17 (2008) 1080-1088.
- [24] A. R. Konicek, D. S. Grierson, P. U. P. A. Gilbert, W. G. Sawyer, A. V. Sumant, R. W. Carpick, Origin of Ultralow Friction and Wear in Ultrananocrystalline Diamond, *Phys. Rev. Lett.* 100 (2008) 235502-04.
- [25] J. E. Butler, A. V. Sumant, The CVD of Nanodiamond Materials, *Chem. Vap. Deposition* 14 (2008) 145-160.
- [26] J. P. Thomas, H. C. Chen, N. H. Tai, I -N. Lin, Freestanding Ultrananocrystalline Diamond Films with Homo Junction Insulating Layer on Conducting Layer and Their High Electron Field Emission Properties, *ACS Appl Mater Interfaces* 3 (2011) 4007-4013.

- [27] W. Kulisch, C. Petkov, E. Petkov, C. Popov, P. N. Gibson, M. Veres, R. Merz, B. Merz, J. P. Reithmaier, Low temperature growth of nanocrystalline and ultrananocrystalline diamond films: A comparison, *Phys. Status Solidi A* 209 (2012) 1664-1674.
- [28] K. J. Sankaran *et al.*, Improvement in plasma illumination properties of ultrananocrystalline diamond films by grain boundary engineering, *J. Appl. Phys.* 114 (2013) 054304-11.
- [29] K. J. Sankaran *et al.*, Improvement in Tribological Properties by Modification of Grain Boundary and Microstructure of Ultrananocrystalline Diamond Films, *ACS Appl. Mater. Interfaces* 5 (2013) 3614-3624.
- [30] A. Saravanan *et al.*, Fast growth of ultrananocrystalline diamond films by bias-enhanced nucleation and growth process in CH₄/Ar plasma, *Appl. Phys. Lett.* 104 (2014) 181603-5.
- [31] C. S. Wang, H. C. Chen, H. F. Cheng, I –N. Lin, Origin of platelike granular structure for the ultrananocrystalline diamond films synthesized in H₂ - containing Ar / CH₄ plasma, *J. Appl. Phys.* 107 (2014) 034304-7.
- [32] H. Zeng *et al.*, Boron-doped ultrananocrystalline diamond synthesized with an H-rich/Ar-lean gas system, *Carbon* 84 (2015) 103-117.
- [33] K. J. Sankaran, K. Panda, B. Sundaravel, H. –C. Chen, I –N. Lin, C. –Y. Lee, N. –H. Tai, Engineering the Interface Characteristics of Ultrananocrystalline Diamond Films Grown on Au-Coated Si Substrates, *ACS Appl. Mater. Interfaces* 4 (2012) 4169-4176.
- [34] J. P. Thomas *et al.*, Preferentially Grown Ultrananocrystalline Diamond and n-Diamond Grains on Silicon Nanoneedles from Energetic Species with Enhanced Field-Emission Properties, *ACS Appl. Mater. Interfaces* 4 (2012) 5103-5108.
- [35] K. J. Sankaran, H. –C. Chen, K. Panda, B. Sundaravel, C. –Young Lee, N. –H. Tai, I –N. Lin, Enhanced Electron Field Emission Properties of Conducting Ultrananocrystalline Diamond Films after Cu and Au Ion Implantation, *ACS Appl. Mater. Interfaces* 6 (2014) 4911-4919.
- [36] K. J. Sankaran, K. Panda, B. Sundaravel, N. H. Tai, I –N. Lin, Enhancing electrical conductivity and electron field emission properties of ultrananocrystalline diamond films by copper ion implantation and annealing, *J. Appl. Phys.* 115 (2014) 063701-7.

- [37] K. J. Sankaran *et al.*, Electron Field Emission Enhancement of Vertically Aligned Ultrananocrystalline Diamond-Coated ZnO Core–Shell Heterostructured Nanorods, *Small* 10 (2014) 179-185.
- [38] Y. Tzeng, S. Yeh, W. C. Fang, Y. Chu, Nitrogen-incorporated ultrananocrystalline diamond and multi-layer-graphene-like hybrid carbon films, *Sci. Rep.* 4 (2014) 4531.
- [39] S. C. Lin *et al.*, The microstructural evolution of ultrananocrystalline diamond films due to P ion implantation and annealing process-dosage effect, *Diam. Relat. Mater.* 54 (2015) 47-54.
- [40] K. Panda, E. Inami, Y. Sugimoto, K. J. Sankaran, I –Nan Lin. Straight imaging and mechanism behind grain boundary electron emission in Pt-doped ultrananocrystalline diamond films. *Carbon* 111 (2017) 8-17.
- [41] A. Saravanan, B. R. Huang, K. J. Sankaran, G. Keiser, J. Kurian, N. H. Tai, I. N. Lin, Structural modification of nanocrystalline diamond films via positive/negative bias enhanced nucleation and growth processes for improving their electron field emission properties, *J. Appl. Phys.* 117 (2015) 215307-11.
- [42] D. M. Gruen, S. Liu, A. R. Krauss, X. Pan, Buckyball microwave plasmas: Fragmentation and diamond-film growth, *J. Appl. Phys.* 75 (1994) 1758-1763.
- [43] P. Kovarik, E. B. D. Bourdon, R. H. Prince, Electron-energy-loss characterization of laser-deposited *a*-C, *a*-C:H, and diamond films, *Phys. Rev. B* 48 (1993) 12123-12129.
- [44] W. A. Yarbrough, R. Messier, Current issues and problems in the chemical vapor deposition of diamond, *Science* 247 (1990) 688-696.
- [45] R. J. Nemanich, J. T. Glass, G. Lucovsky, R. E. Shroder, Raman scattering characterization of carbon bonding in diamond and diamondlike thin films, *J. Vac. Sci. Technol. A* 6 (1988) 1783-1787.
- [46] R. E. Shroder, R. J. Nemanich, J. T. Glass, Analysis of the composite structures in diamond thin films by Raman spectroscopy, *Phys. Rev. B* 41 (1990) 3738-3745.
- [47] A. C. Ferrari, J. Robertson, Origin of the 1150cm^{-1} Raman mode in nanocrystalline diamond, *Phys. Rev. B* 63 (2001) 121405-5.
- [48] I. Jiménez, M. M. García, J. M. Albella, L. J. Terminello, Orientation of graphitic planes during the bias-enhanced nucleation of diamond on silicon: An x-ray absorption near-edge study, *Appl. Phys. Lett.* 73 (1998) 2911-2913.

- [49] J. Birrell, J. E. Gerbi, O. Auciello, J. M. Gibson, J. Johnson, J. A. Carlisle, Interpretation of the Raman spectra of ultrananocrystalline diamond, *Diam. Relat. Mater.* 14 (2005) 86-92.
- [50] R. Haubner, M. Rudigier, Raman characterisation of diamond coatings using different laser wavelengths, *Physics Procedia* 46 (2013) 71-78.
- [51] S. C. Ray, I –N. Lin, Ferroelectric behaviours of ultra-nano-crystalline diamond thin films, *Surf. Coat. Technol.* 271 (2015) 247-250.

Authors' biography:

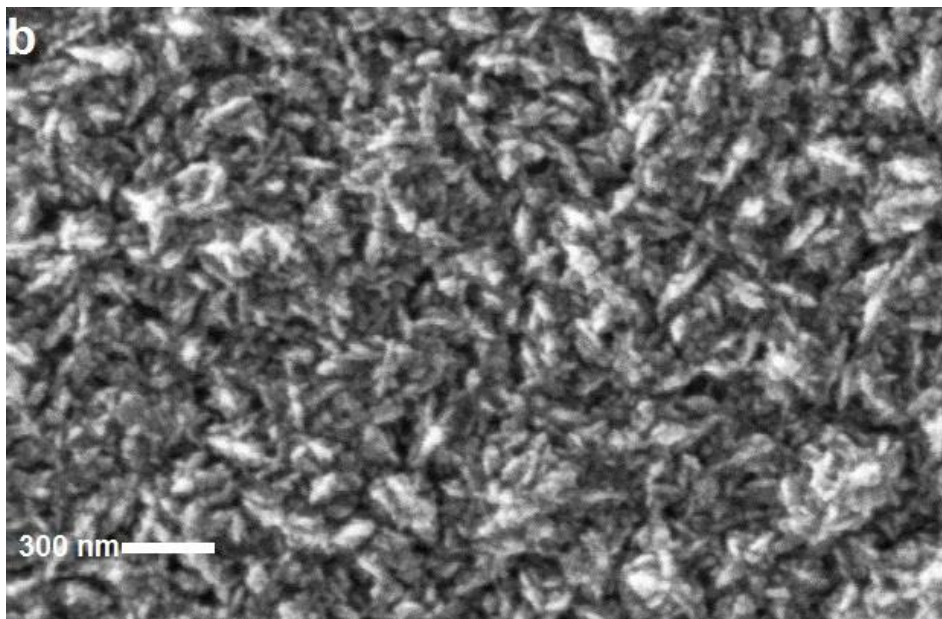
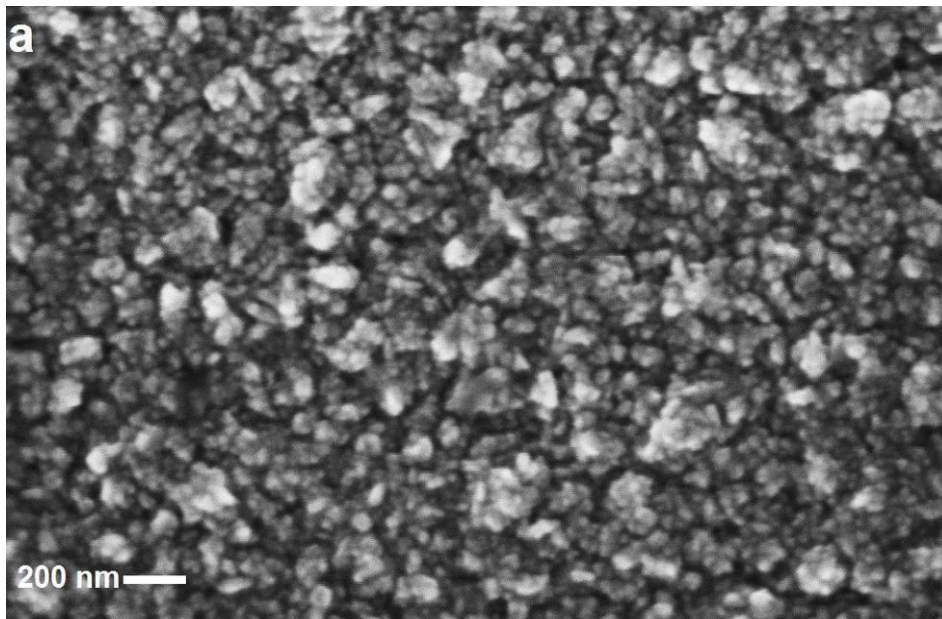


Mubarak Ali graduated from University of the Punjab with B.Sc. (Phys& Maths) in 1996 and M.Sc. Materials Science with distinction at Bahauddin Zakariya University, Multan, Pakistan (1998); thesis work completed at Quaid-i-Azam University Islamabad. He gained Ph.D. in Mechanical Engineering from Universiti Teknologi Malaysia under the award of Malaysian Technical Cooperation Programme (MTCP;2004-07) and postdoc in advanced surface technologies at Istanbul Technical University under the foreign fellowship of The Scientific and Technological Research Council of Turkey (TÜBİTAK; 2010). He completed another postdoc in the field of nanotechnology at Tamkang University Taipei (2013-2014) sponsored by National Science Council now M/o Science and Technology, Taiwan (R.O.C.). Presently, he is working as Assistant Professor on tenure track at COMSATS Institute of Information Technology, Islamabad campus, Pakistan (since May 2008) and prior to that worked as assistant director/deputy director at M/o Science & Technology (Pakistan Council of Renewable Energy Technologies, Islamabad; 2000-2008). He was invited by Institute for Materials Research (IMR), Tohoku University, Japan to deliver scientific talk on growth of synthetic diamond without seeding treatment and synthesis of tantalum carbide. He gave several scientific talks in various countries. His core area of research includes materials science, physics & nanotechnology. He was also offered the merit scholarship (for PhD study) by the Government of Pakistan but he couldn't avail. He is author of several articles published in various periodicals (<https://scholar.google.com.pk/citations?hl=en&user=UYivhDwAAAAJ>).



I-Nan Lin is a senior professor at Tamkang University, Taiwan. He received the Bachelor degree in physics from National Taiwan Normal University, Taiwan, M.S. from National Tsing-Hua University, Taiwan, and the Ph.D. degree in Materials Science from U. C. Berkeley in 1979, U.S.A. He worked as senior researcher in Materials Science Centre in Tsing-Hua University for several years and now is faculty in Department of Physics, Tamkang University. Professor Lin has more than 200 referred journal publications and holds top position in his university in terms of research productivity. Professor I-Nan Lin supervised several PhD and Postdoc candidates around the world. He is involved in research on the development of high conductivity diamond films and on the transmission microscopy of materials.

Supplementary Materials:



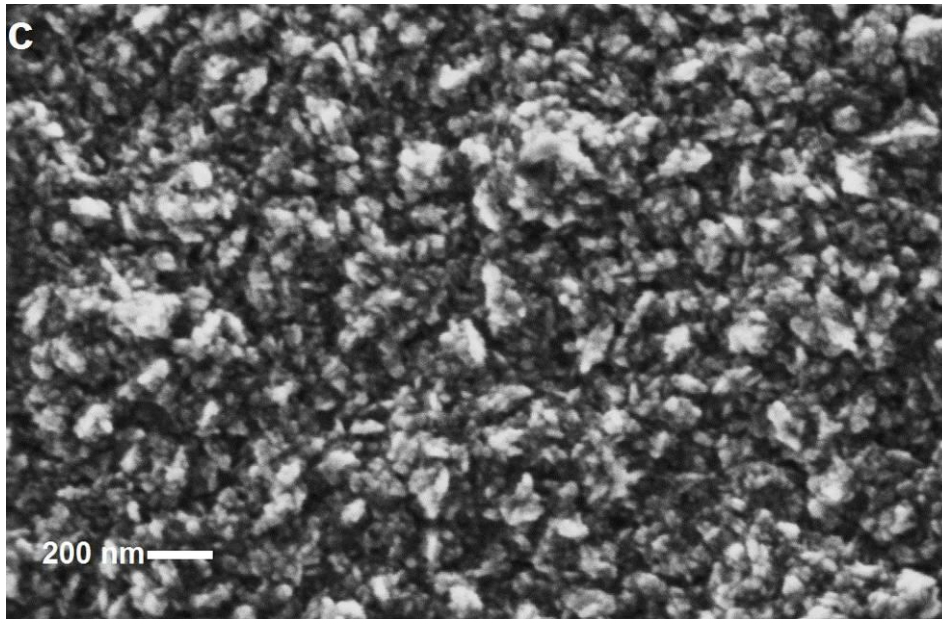


Figure S1: Surface morphology of 'tiny grains carbon films' synthesized at chamber pressure (a) 100 torr, (b) 150 torr, and (c) 200 torr; total mass flow rate: 200 sccm (6% H₂, 1 % CH₄ and 93 % argon, Ar: CH₄: H₂ = 186:2:12), microwave power: 1400 (in watts) and deposition time: 60 minutes.

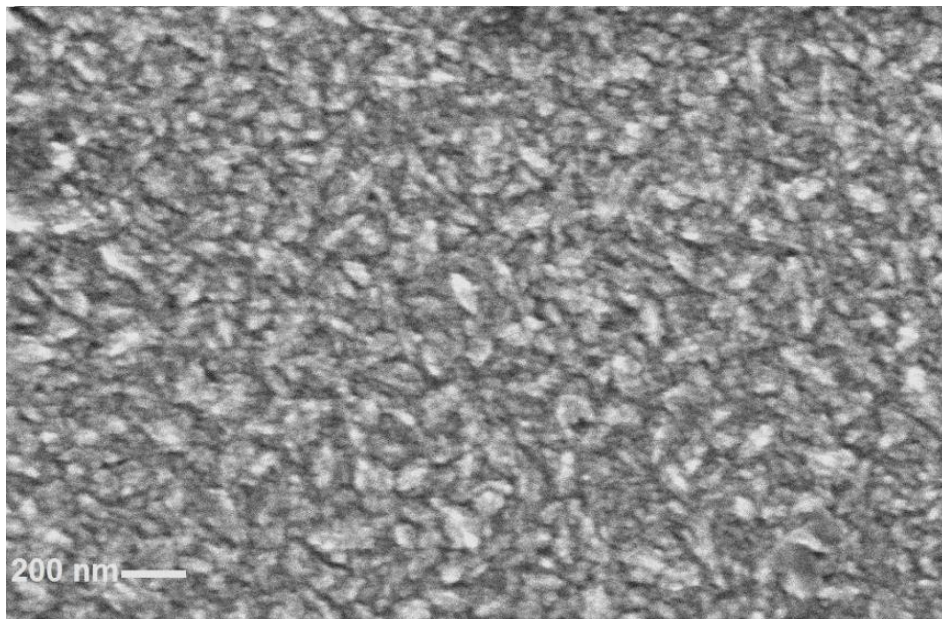


Figure S2: Surface morphology of 'tiny grains carbon film' synthesized at chamber pressure 150 torr; total mass flow rate: 200 sccm (0% H₂, 2 % CH₄ and 98 % argon, Ar: CH₄: H₂ = 196:4:0), microwave power: 1100 (in watts) and deposition time: 60 minutes.

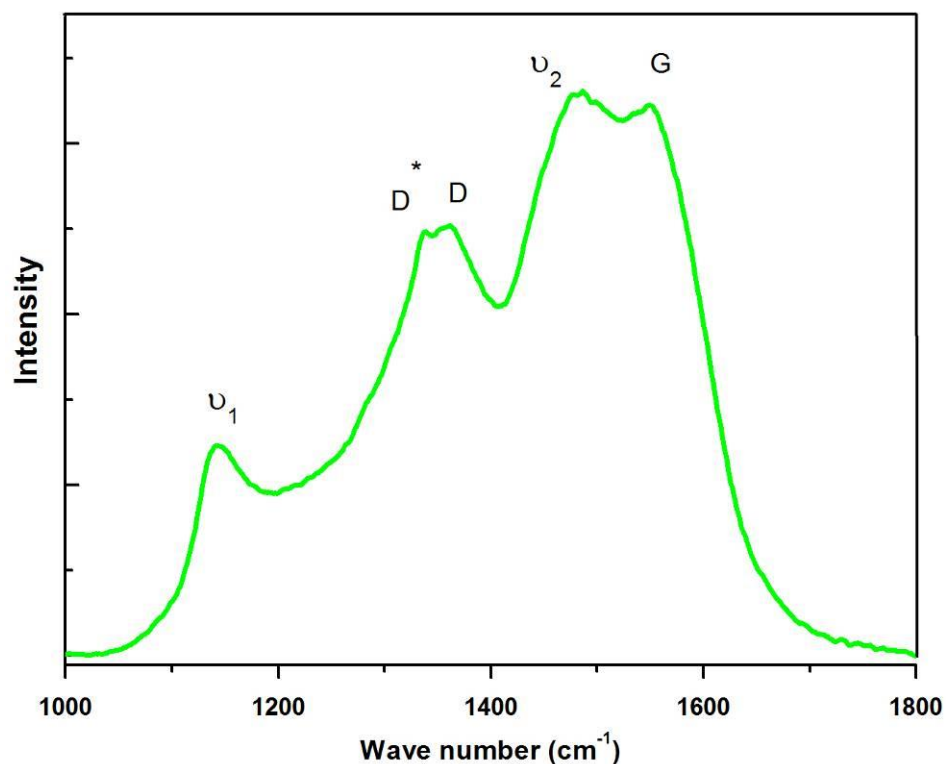
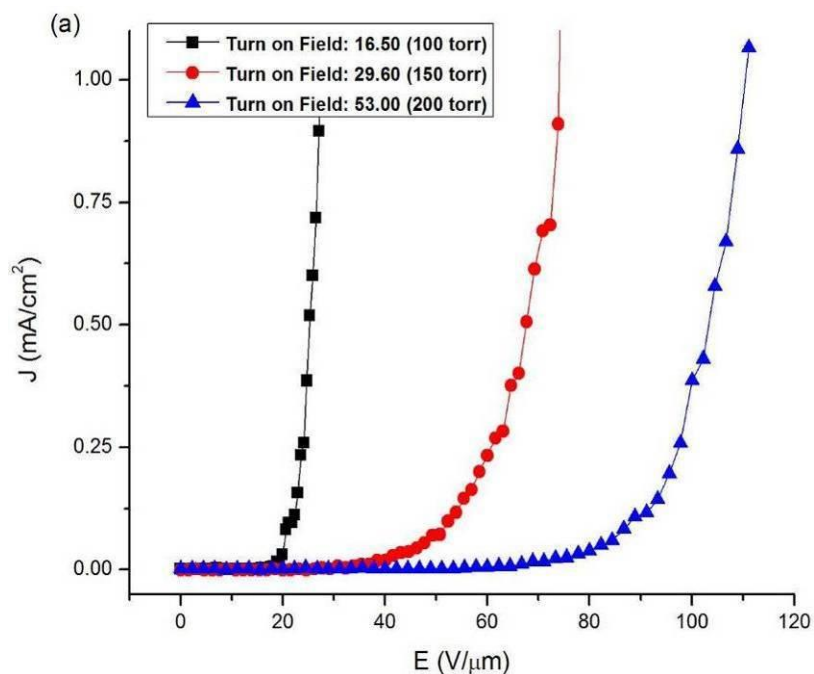


Figure S3: Raman spectrum of 'tiny grains carbon film' synthesized at chamber pressure 150 torr; total mass flow rate: 200 sccm (0% H₂, 2 % CH₄ and 98 % argon, Ar: CH₄: H₂ = 196:4:0), microwave power: 1100 (in watts) and deposition time: 60 minutes (v₁: ~ 1145 cm⁻¹, D*: ~ 1310 cm⁻¹, D: 1332 cm⁻¹, v₂: ~ 1480 cm⁻¹, G: ~ 1580 cm⁻¹).



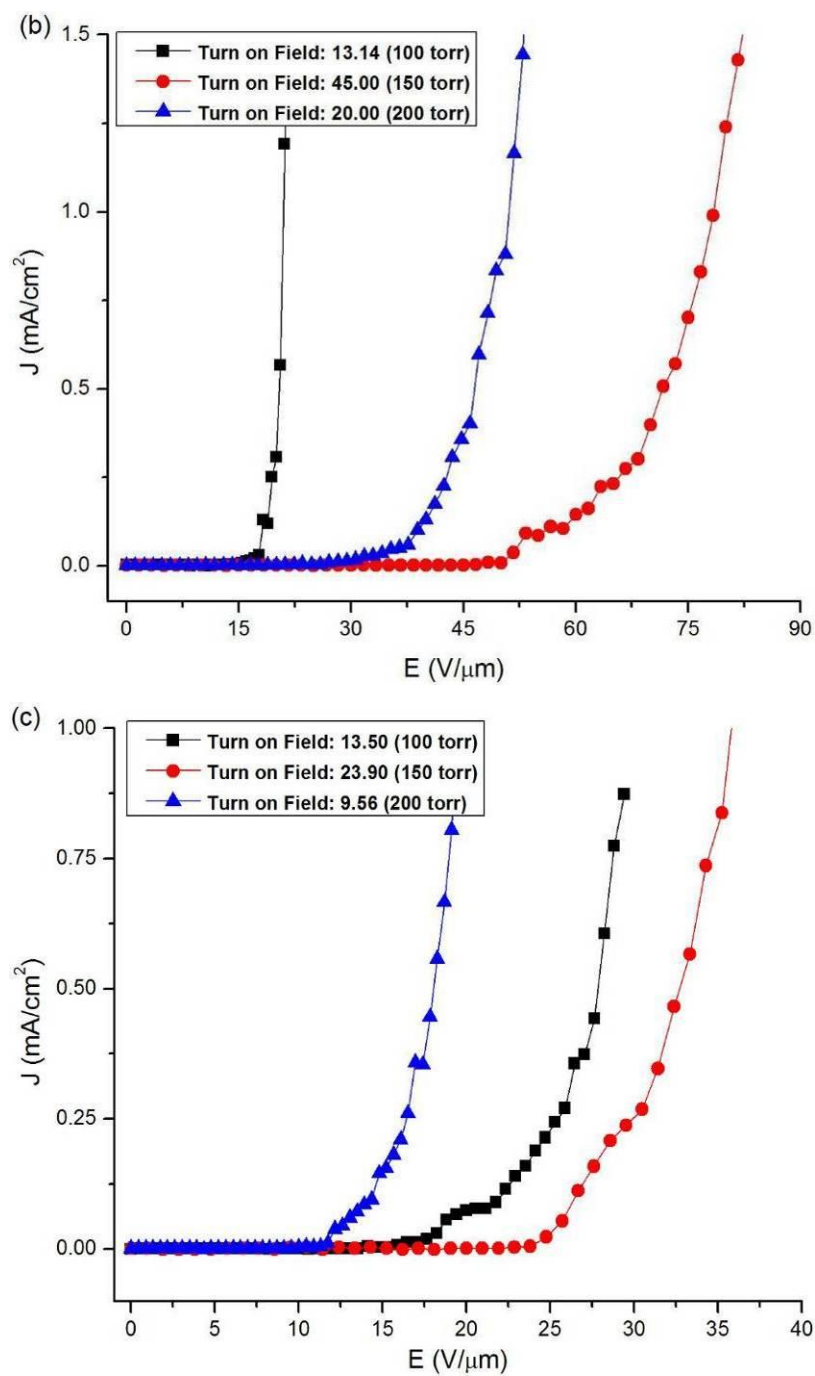


Figure S4: Field emission current density as a function of applied field of 'tiny grains carbon films' synthesized (a) without H₂, (b) with 3 % H₂ and (c) with 6 % H₂; 1 % CH₄, total mass flow rate: 200 sccm, microwave power: 1200 (in watts) and deposition time: 60 minutes.

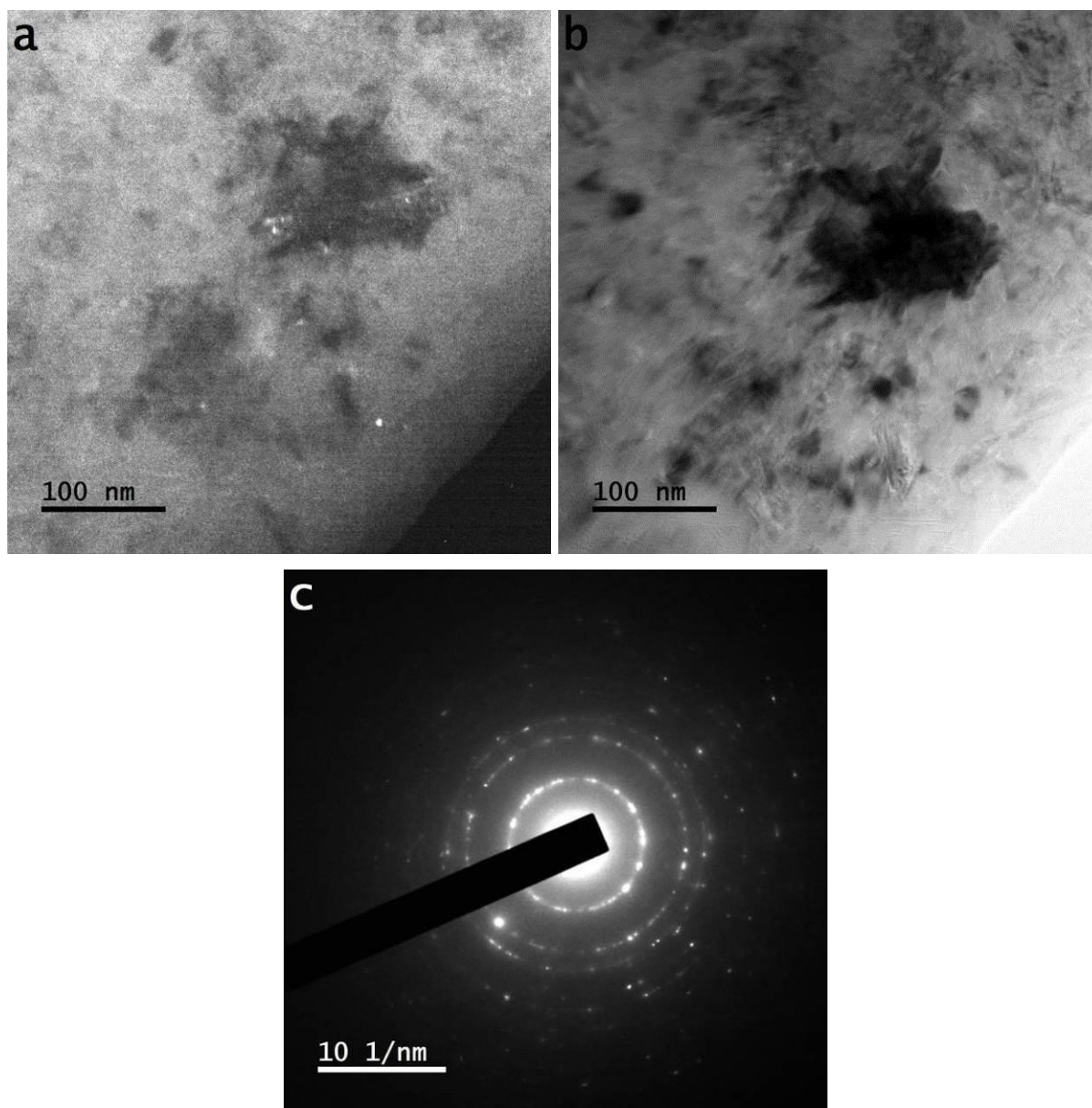


Figure S5: (a) Dark field transmission microscope image (b) bright field transmission microscope image and (c) SAPR pattern of 'tiny grains carbon film' synthesized at chamber pressure: 100 torr, total mass flow rate: 200 sccm (6% H₂, 1 % CH₄ and 93 % argon), microwave power: 1400 watts (in watts) and deposition time: 60 minutes.

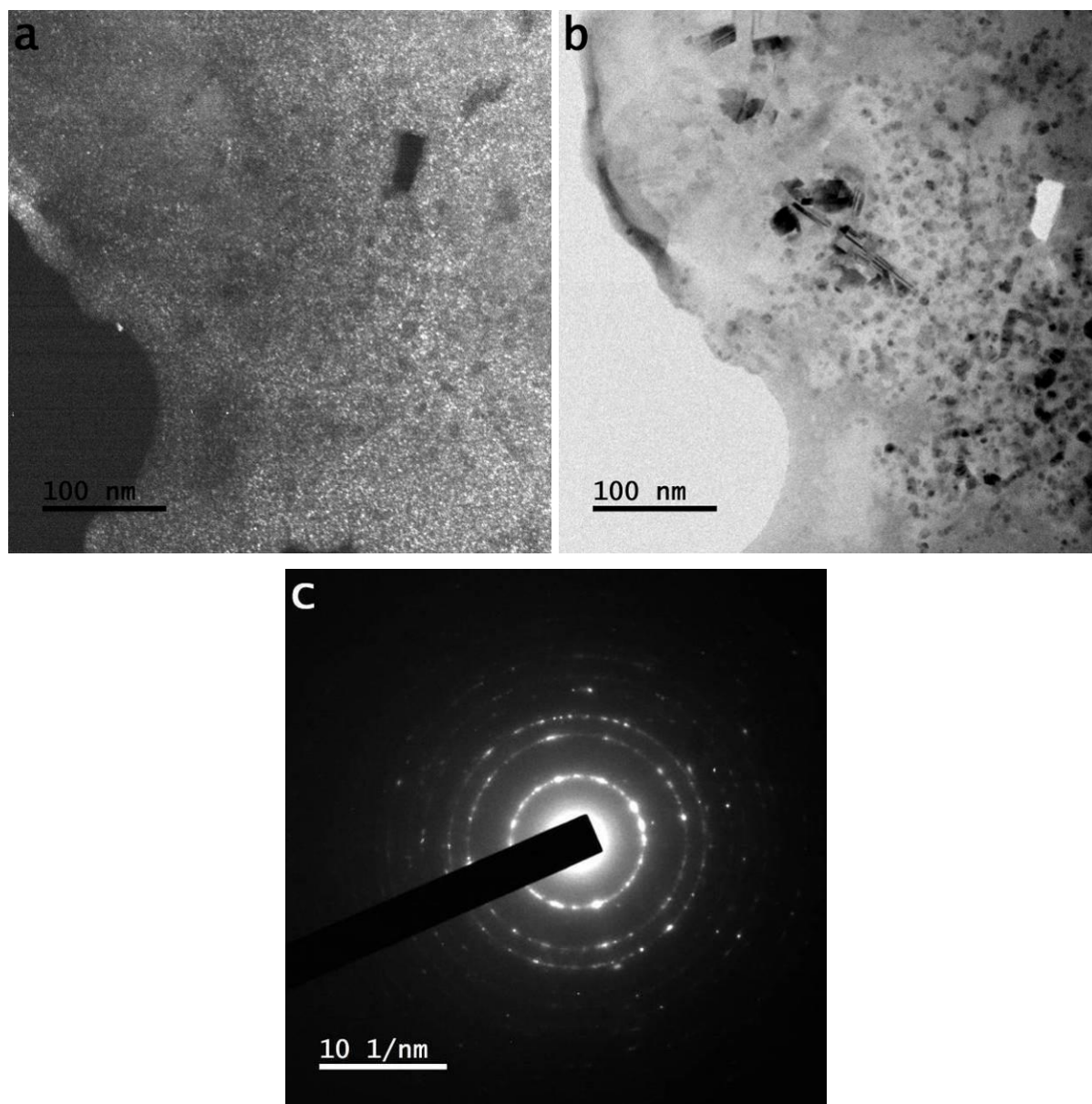


Figure S6: (a) Dark field transmission microscope image (b) bright field transmission microscope image and (c) SAPR pattern of 'tiny grains carbon film' synthesized at chamber pressure: 200 torr, total mass flow rate: 200 sccm (6% H₂, 1 % CH₄ and 93 % argon), microwave power: 1400 (in watts) and deposition time: 60 minutes.

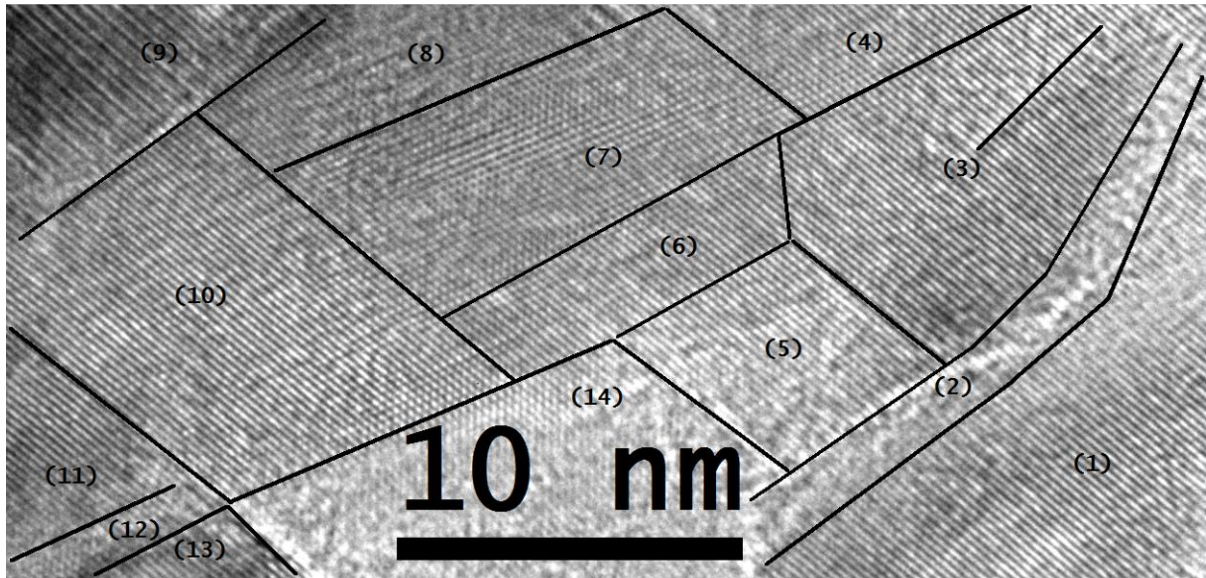


Figure S7: High-resolution transmission microscope image of 'tiny grains carbon film' synthesized at chamber pressure 100 torr shows different state of carbon atoms along with elongated graphite structure tiny grains; total mass flow rate: 200 sccm (6% H₂, 1 % CH₄ and 93 % argon), microwave power: 1400 (in watts) and deposition time: 60 minutes.